Sixth International Conference on Durability of Concrete Structures **Paper Number TIM03**
18 - 20 July 2018
University of Leeds, Leeds, West Yorkshire, LS2 9JT, United Kingdom

Design of an *in situ* steady-state permeability test to determine the air permeability of covercrete

K. Yang and P.A.M. Basheer
School of Civil Engineering, University of Leeds, UK

A.E. Long and S. Nanukuttan
School of the Natural and Built Environment, Queen's University Belfast, UK

C. Yang
College of Materials Science and Engineering, Chongqing University, China

Y. Wang
School of Civil Engineering, Shenzhen University, China

S. Mu
State Key Laboratory of High Performance Civil Engineering Materials,
Jiangsu Sobute New Materials Co., Ltd, Nanjing, China

ABSTRACT

An in situ permeability test method that does not require assumptions for the uni-directional flow has been developed to determine the air permeability coefficient of the near surface concrete. The proposed method involves applying a constant pressure head to a surface mounted ring and measuring steady state air flow rates. The analysis is based on modification of the flow net theory, which needs a calibration factor accounting for the influence of specimen and ring geometries. Effects of test area, width of seal, depth and width of test specimen were investigated using numerical simulation of air flow. The results indicated that the value of the calibration is very sensitive to change of testing area which needs to be corrected for a specimen with a depth less than 50 mm. The experimental studies suggest the duration to achieve the steady state depends on the quality of the concrete tested and the applied pressure. The results indicated that the test method is capable of identifying the difference in quality of concretes.

Keywords: flow net, steady-state state, *in situ* air permeability test, covercrete

1.0 INTRODUCTION

The assessment of permeability is of great importance for many scientific and practical problems associated with the use of concrete in many construction projects, *e.g.* concrete property optimisation, structural quality control, service life prediction. *In situ* air permeability test methods offer considerable advantages in terms of many criteria deemed to be important for field assessment of permeability and are rapidly becoming a commonly accepted method for determining permeation properties of structural concrete. In this respect, they have proven to be useful for characterising site quality and potential durability of concrete in structure (Parrott *et al* 1991; Neves *et al*, 2011; Yang *et al*, 2014). In addition to this, they are also useful for providing essential input parameters required for most service life prediction models (Imamoto *et al*, 2009; Neves *et al*, 2011; Silva *et al.* 2014).

Following the early work of Figg (1973) in 1970s, numerous air permeability methods have been developed, which can be grouped under surface mounted tests and drill-hole tests. In spite of remarkable variations of these methods, such as testing procedures, capabilities, and complexity, the fundamental principle of these methods is the same, which is based on non-steady state flow analysis for reasons of simplicity. Semi-empirical calculations based on measurements carried out allow the determination of the air permeability in a fairly consistent quantitative way. However, in most cases, it is only possible to obtain a permeability index, and the coefficient of air permeability cannot be estimated due to inherent limitations.

The empirical theories assume that the uni-directional flow is reached and all the accessible porosity used in the governing equation is regarded as a constant or embedded into the permeability indicator (Torrent, 1992; Basheer, 2001). Clearly, both these hypothesises cannot be achieved in field measurements and, hence, currently no *in situ* method is available for determining the air permeability coefficient. Although a guard-ring is used

to achieve the uni-directional flow in the test region and to increase the effective test region (Hall, 1989; Torrent, 1992; Claisse *et al*, 1999), it is still debatable whether its benefits over other test arrangements justify the higher complexity associated with the test set up using guard rings. Yang *et al.* (2015-a) have shown that the flow features are significantly affected by various test set up as well as test location related factors and even under the best circumstances, only the central portion of the guard ring approximates a true one-dimensional flow system.

The steady-state analysis, normally not taken in to consideration in field test techniques, has many scientific and technological advantages. It minimises the effect of both the multi-directional flow and variations in porosity with depth, both of which avoid two unreliable assumptions (Adams, 1986; Bamforth, 1987; Basheer, 2001; Yang *et al*, 2015-b). Currently, most steady-state field test methods are water permeability tests. Whiting *et al* (1992) developed a field test to measure the steady-state air flow rate under vacuum, but no analytical solution to obtain an air permeability coefficient was given. Against these backgrounds, it was established that a rapid, non-destructive, *in situ* air permeability test was needed.

Therefore, the objective of this study was to develop a steady state air permeability test, by putting emphasis on determining the permeability coefficient, which incorporates the advantages of current field test methods while eliminating their limitations.

2.0 GOVERNING EQUATION TO DETERMINE THE AIR PERMEABILITY COEFFICIENT

The flow net theory, which was used to determine the coefficient of water permeability of concrete in the CLAM test (Adams, 1986), is sufficiently versatile theory to be applied to the steady-state air permeability test. The method involves the establishment of a flow net that consists of equipotential lines and flow lines, as indicated in Fig.1.

The relationship between the permeability coefficient and the steady state flow rate can be expressed by:

$$K_{air} = q \times \frac{1}{2\pi h_t} \times \frac{n_d}{n_f} \times \frac{l}{rb} = q \times C \quad (1)$$

where K_{air} is the air permeability coefficient (m/s); q is the steady-state air flow (m^3/s); h_t is the head applied (m); n_f is the number of paths (flow channels); n_d is the number of equipotential drops; r is the distance normal to symmetry axis (m); b is the width of flow path (m); l is the distance between equipotential lines (m); $\frac{1}{2\pi h_t} \times \frac{n_d}{n_f} \times \frac{l}{rb}$ is considered as the calibration factor (C), which is a function of only the flow geometry. Verification of the flow net theory has been previously reported by several researchers (Adams, 1986; Bamforth, 1987; Yang *et al*, 2015).

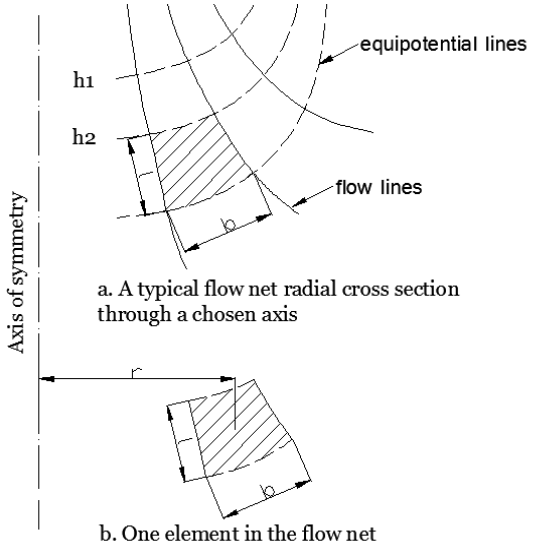

Fig. 1. Illustration of determining the calibration factor for the flow net

3.0 FLOW SIMULATION TO EVALUATE THE VALUE OF CALIBRATION FACTOR

The flow simulation is not only helpful to optimise the instrument design, but also useful to establish approaches to interpret test results. The finite element analysis (FEA) provides a valuable means to achieve this (Yang *et al*, 2015-a). Against these backgrounds, the air flow simulation was carried out to clarify the influence of geometric configurations of the specimen and the instrument on the flow net. More specifically, the following four factors are taken into account (refer to Fig.2 for identifying the parameters): 1) depth of the specimen (d_{sp}); 2) width of the specimen (w_{sp}); 3) radius of the testing area (r_{ta}); 4) size of a flat ring-shaped seal (S_w) which refers the width of the seal around the central test region.

A factorial experiment design was done to investigate the effect of the above four factors, details of which are summarised in Table 1 and sixteen models were built. In developing the flow net for a given condition, the orthogonality condition must be satisfied and producing an acceptable solution is largely a matter of trial and error, which, in turn, is a function of the experience and patience (Adams, 1986; Bamforth, 1987; Arbaoui, 1988). Figure 2 illustrates the input boundary conditions and the output of the simulation. On the basis of the simulated flow net, the calibration factor (C) was evaluated.

Table 1. Design of factorial experiment to assess the influence of different factors on calibration factor

Factor	d_{sp} (mm)	w_{sp} (mm)	r_{ta} (mm)	S_w (mm)
"+"	100	150	25	10
"-"	50	100	50	30

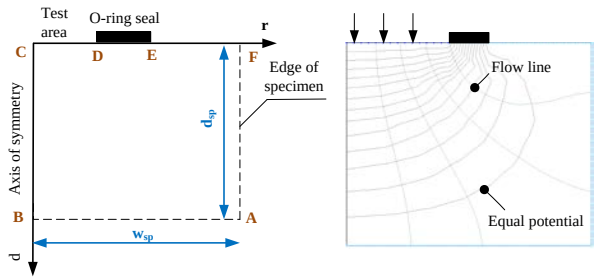

(a) Geometry considered for air flow models

(b) Output of air simulation model

Fig.2 Configuration of flow models to study influence of configuration on calibration factor

Table 2 summarises results of the factorial analysis. The statistical analysis reveals that the effect of the radius has a significant influence on calibration factor; the greater the radius, the lower the calibration factor. As indicated in Fig.1, an increase in the radius of the test area would increase the distance normal to symmetry axis (r) and the width of the flow path (b), which naturally leads to an overall decrease of l/rb. The results also indicate that within the two levels of the factors investigated, the only factor which was found to be significant is the radius of the test area, while the calibration factor is not strongly affected by changes of other factors. As indicated in Table 2, the interactions between different factors are not found to be significant (Rawlings *et al*, 1998). On the basis of the results obtained in this study and previous research reported by Yang *et al.* (2015-b) , it is decided to design the instrument with the 25 mm test radius to eliminate the heterogeneous nature of concrete. In addition, to avoid the influence of top layer, the size of a flat ring-shaped seal is specified as 30 mm to force air passing through the full cover zone (Schonlin *et al*, 1987; Parrott *et al*, 1991; Torrent, 1992; Whiting *et al*, 1992).

Once the geometry parameters of the test instrument were determined, further investigations were carried out to refine the influence of boundary conditions of the specimen. It was intended to estimate potential correction factors under certain practical conditions, e.g. assessment of thin layers or close to the edge of structural elements. Therefore, another 11 models were built to examine the influence of specimen depth and distance to the outer side of test specimens. Calibration coefficients obtained from the flow simulation results are displayed in Fig. 3.

Figure 3-a gives the relationship between the calibration factor and the depth. Obviously, an increase in specimen depth caused an increase in

Table 2. Estimated effects and coefficients for calibration factor

Term	Effect	Coefficient	Standard error of coefficient	P-Value
Constant		0.0325	0.0008	0.016*
r_{ta}	-0.027	-0.013	0.0008	0.038*
S_w	0.004	0.0019	0.0008	0.254
d_{sp}	0.003	0.0017	0.0008	0.287
w_{sp}	-0.002	-0.001	0.0008	0.525
$r_{ta}\times S_w$	-0.002	-0.001	0.0008	0.429
$r_{ta}\times d_{sp}$	0.001	0.0004	0.0008	0.698
$r_{ta}\times w_{sp}$	0.0001	0.0001	0.0008	0.952
$S_w\times d_{sp}$	-0.000	-0.000	0.0008	0.929
$S_w\times w_{sp}$	0.003	0.0014	0.0008	0.327
$d_{sp}\times w_{sp}$	0.001	0.0007	0.0008	0.553
$r_{ta}\times S_w\times d_{sp}$	0.0002	0.0001	0.0008	0.926
$r_{ta}\times S_w\times w_{sp}$	0.0007	0.0004	0.0008	0.737
$r_{ta}\times d_{sp}\times w_{sp}$	-0.001	-0.001	0.0008	0.600
$r_{ta}\times S_w\times d_{sp}\times w_{sp}$	0.001	0.0003	0.0008	0.743

* significant effect, p-value: 1%-5%

calibration factor, but reached a relatively constant value (0.051 mm^{-1}) beyond 50 mm. This is mainly due to rapid changes in the relative proportion of the horizontal flow lines and the growth of the *l* component (the distance between equipotential lines), both yielding a higher calibration factor. This means a higher pressure gradient and, hence, a higher proportion of horizontal flow lines in these cases.

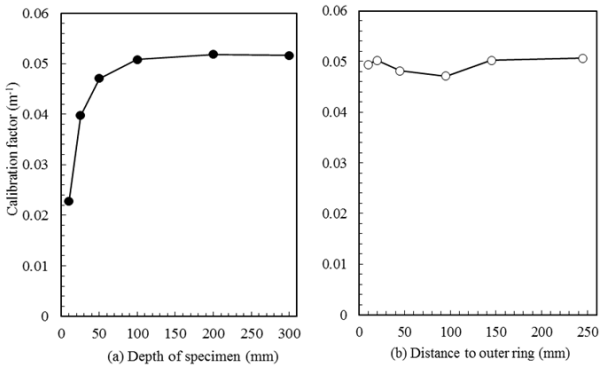

Fig.3. Calibration factor under different specimen depths and distances to outer side of the seal

The above result agrees well with the previous findings by Bamforth (1987) and Arbaoui (1988). Figure 3-b plots the calibration factor against the distance between the test area and the outer edge. Note that in these figures, the depth was kept at a constant value (100 mm) to avoid additional variations in the calibration factor due to this factor. It was found that the distance to the outer side of the test specimen did not have a noticeable effect on the flow net in comparison to the effect of the specimen depth. This trend is also clearly reflected in low variations in the calibration factors. Parrott and Hong (1991) investigated the effective testing volume of concrete and the air permeated area was observed

from the bubbling region on the surface. They also highlighted that the influencing region is mainly about 20 mm around the testing area, which is similar to the results here. For this reason, it was concluded that there is no need to correct the calibration factor for the distance from the inner test region to the outer edge of the specimen.

4.0 DESIGN OF THE *IN SITU* AIR PERMEABILITY TEST INSTRUMENT

The air permeability is calculated according to the flow net theory, which requires the value of the steady-state air flow rate, as highlighted in Eq. 1. To verify the approach to determine the air permeability coefficient, it was necessary to construct a test prototype and obtain the value of the steady state air flow rate. Figure 4 shows the air permeability test instrument, which is similar to the high-pressure water permeability test reported by Yang *et al.* (2015). As indicated in results of the air flow simulation, the testing area was chosen as circular with a radius of 25 mm, offering a representative testing area for most structural concrete (Torrent 1992; Dhir *et al.*, 1995). This was achieved by using a 110 mm diameter aluminium plate fitted with a 5 mm thick natural rubber ring that isolated a circular flow area of 25 mm internal diameter.

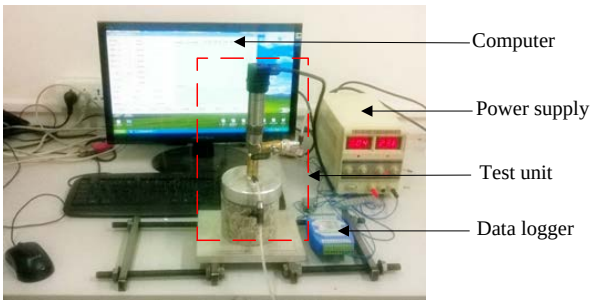

Fig.4 Test set up of the new laboratory air permeability test device

5.0 EXPERIMENTAL PROGRAMME

The experimental work was intended to verify the proposed theory under different testing conditions and assess the performance of the constant head air permeability test instrument. To achieve this objective, the influence of test pressure on duration to reach a steady state flow rate was investigated first, following by establishing the relationship between the test pressure and the steady-state flow rate.

5.1 Preparation of the Test Specimens

The concrete investigated was manufactured with a water-cement ratio of 0.35 and a mix proportion of 1:1.44:2.56 between cement, sand and coarse aggregate. The concrete was manufactured with CEM I, 42.5N Portland cement, medium natural sand (fineness modulus: 2.60, specific gravity: 2.52), and 10mm and 20 mm size basalt coarse aggregate (specific gravity: 2.65) in a 1:1 proportion by weight. Dried aggregates were used and a predetermined allowance for their water absorption was made to the total water used in the mix. A polycarboxylic acid based superplasticiser was used to achieve the target workability, measured in slump of 210 mm. The mixing was carried out according to BS-1881: part 125 (1986). After mixing, the slump and air content were determined according to GB-50082 (2009), which were 210 mm and 1.6% respectively.

The test specimens were blocks of size 300×250×150 mm and the proposed air permeability tests were carried out on the 300×250 mm mould finished surface. After compaction, the specimens were immediately covered with plastic sheets to prevent the evaporation of water from the freshly placed concrete. The blocks were removed from their mould after 1 day and were cured until the age of 90 days by following the two procedures below:

1) Air cured (AC): air-storage in a controlled environment (20 ± 2 ^{o}C, 50 ± 10% RH) after demoulding.
2) Sealed cured (SC): wrapped in plastic sheets and moved to a temperature controlled environment (20 ± 2 ^{o}C) after 3-day water curing at a water temperature of 20 ± 1 ^{o}C.

Two curing regimes were designed to offer different permeability properties, especially for the near surface region. Note that prior to carrying out air permeability measurements, the slabs were dried in an oven at 40 ^{o}C for 28 days after curing in order to remove the influence of moisture on the results (Torrent, 1992; Parrott, 1994; Yang *et al*., 2013).

5.2 Proposed new air permeability test

The test set up shown in Fig. 4 was used to carry out the air permeability test. At the beginning of measurements, the test head was clamped onto a given specimen. The test system was then pressurised using compressed air. Once the pressure in the test system was slightly above pre-specified pressure, initial pressurisation was considered complete and a volume reading was recorded as the initial value (t=0 min). As gas flowed into the concrete under examination, pressure inside the test head decreased. To maintain a pressure bar, equipment pistons were advanced and the volume of gas recorded every minute. The test duration is selected to be 60 mins. The instrument has two distinctive features, including maintaining the constant testing pressure and measuring the flow rate accurately.

6.0 RESULTS AND DISCUSSION

6.1 The effect of test pressure and curing regime on air flow response

To identify the influence of test pressure on the air flow, the flow rates were monitored continuously, which were used to identify the duration at which the steady state was achieved. Figure 5 shows the plot of the recorded air flow rates under different pressure levels, while each data point represents the average value of 3 replicates at different locations. As shown in Fig. 5, strong fluctuations of air flow are observed at the beginning which is generally considered as the non-steady state. Another feature is that the length of the non-steady state stage mainly depended on the test pressure applied and concrete tested. More specifically, it took 30 minutes to achieve the steady state when the testing pressure was 0.5 bar for the two concretes, while at 1.2 bar the air flow rates became constant within 20 minutes. This means that the increase of test pressure from 0.5 bar to 1.2 bar can significantly shorten the duration to get the steady rate of flow from 30 minutes to 20 minutes. This trend, however, was less pronounced when test pressure was further increased to 2 bar, as the time needed to achieve a steady-state did not show a significant reduction. Steady state flow is obtained when the flow net is established within the test region and it is common that a high pressure can accelerate the process of establishing the flow patterns (Bamforth 1987; Whiting *et al.*, 1992; El-Dieb *et al.*, 1995). As a result, increasing the testing pressure led to the reduction of time needed for a steady state. However, a further decrease was not observed when the pressure was increased from 1.2 bar to 2 bar. It is believed that the duration does not significantly change once the flow pattern is established. In the test carried out for this resaerch, the test area was relatively small and hence, establishing the flow net did not need too much time.

In addition to the test pressure, concrete also affects the duration of establishing a steady state of air flow. When the results in Figs. 5-a and –b are compared, the air flow for AC becomes stable within 10 minutes, whereas the air flow for MC needs around 20 minutes to achieve a similar stage. Various researchers (Arbaoui, 1988; Whiting *et al.*, 1992; Dhir *et al.*, 1995) have shown that a more permeable concrete needs less time to establish a stable flow. In addition, the magnitude of the flow variations positively relates to the values of the corresponding flow rates, which agrees well with previous studies (Basheer *et al.*, 1995; Denarie *et al.*, 2011; Neves *et al.*, 2011).

It may be noted that air can flow deeper under steady state test methods than that under non-steady state test methods. The study of Whiting and Cady (1992) has shown that the air flow can be detected from the 30 mm depth, while the studies carried out by Schonlin *et al.* (1987), Torrent (1992) and Basheer *et al.* (1995) indicate that only the top layer (less than 20 mm) were examined by the non-steady state falling head test methods. Therefore, another advantage of the steady state test is its ability to assess the overall quality of the near-surface concrete.

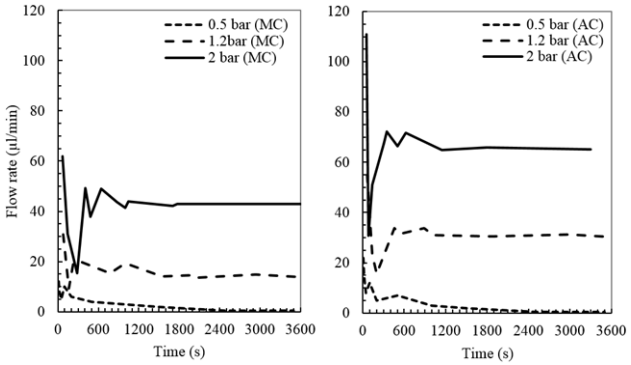

(a) Moist cured (b) Air cured

Fig.5. Air flow rates under different test pressure

Figure 6 shows the steady state flow rate against the test pressure. It can be seen that the steady-state flow rate strongly depends on the concrete curing regimes and increases as the testing pressure increases. As the pressure increases from 0.5 bar to 2 bar, the flow rate of MC increases from 0.42 to 14.12 µl/min, for AC from 0.47 µl/min to 31.50 µl/min. Furthermore, the flow rates of both concretes at 0.5 bar were extremely low, and the difference is not sufficient to distinguish.

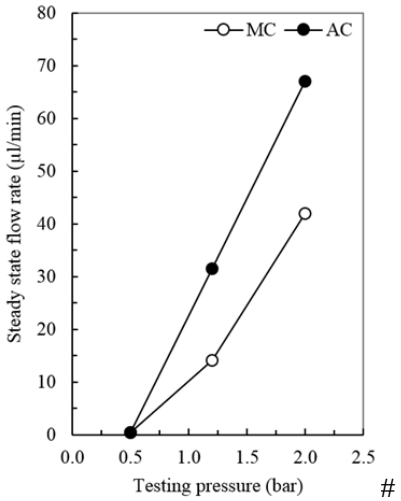

Fig. 6. Relationship between test pressure and steady state air flow rate (The air flow rates at different pressure was converted to the flow rates at 1 atm)

6.2 Relationship between steady-state flow rate and test pressure

the difference between the two concretes. This can be explained because under the low test pressure air moves slowly, which performs more like a molecular diffusion dominated process instead of a pressure dominated process (Basheer *et al.*, 1995; Dhir *et al.*, 1995). The difference in flow rates increases, when the testing pressure is above 1.2 bar. According to

Figs. 5 and 6, the recommended test pressure would be 2 bar, as the final flow rate is high enough that the difference between the two curing regimes can be identified easily.

6.3 Example calculation of coefficient of air permeability using the steady-state air permeability test method

The primary aim of this study was to determine the air permeability coefficient using the proposed approach. The formula (Eq. 2) represents the relationship between air permeability coefficient and steady state air flow rate. To illustrate the procedure, an example of calculation is provided below:

- Environmental conditions in the laboratory: Temperature 21.5 ^{o}C; Relative humidity 62%.
- Curing regime: air cured (AC).
- Initial moisture condition: 40^{o}C dried for 28 days
- Age of concrete: 118 days [curing (90 days) + drying (28 days)]
- Test parameters:

Radius of the test area: 0.025 m

Calibration factor: $\frac{n_d}{n_f}\times\frac{l}{rb}=0.051$ m^{-1} determined from the flow net

- Pressure applied: H = 2 bar (20.4 m)
- Steady state flow rate:

Q_{air}=66.95×10^{-9} m^3/min=1.116×10^{-9} m^3/s.

- Calculation of the air permeability:

$$K_{air}=Q_{air}\times\frac{1}{2\pi h_t}\times\frac{n_d}{n_f}\times\frac{l}{rb}=\frac{1.116\times10^{-9}}{2\times3.14\times20.4}\times0.051=4.443\times10^{-13} \quad (2)$$

7.0 CONCLUSIONS

In this study, a steady-state field test was developed to assess the air permeability of near surface concrete. On the basis of numerical simulation and experimental results, the following conclusions have been drawn:

1) The calibration factor is extremely sensitive to a change of the testing area, which defines the overall flow area, while other factors, including the size of the seal, the thickness of the specimen and the width of the specimen, do not affect the calibration factor significantly.
2) The calibration factor increases as the thickness of the specimen increases and, hence, correction of the calibration factor should be applied to assess the air permeability. However, the value of calibration factor becomes constant (0.051 m^{-1}), if the depth of the specimen is above 50 mm. It is also noted that the distance to the outer side of the seal does not have a significant influence on the calibration factor.
3) Two stages of air flow can be identified from the experiments: (a) Non-steady state stage, marked by a significant fluctuation of flow rate; (b) Steady state stage, shown as a nearly constant flow rate. The duration to obtain a steady air flow rate depends on the pressure applied and the quality of concrete investigated. In addition, flow rates stabilised around 15 minutes, suggesting that a site measurement can be completed within 20 minutes.
4) The steady air flow rate is nearly proportional to the test pressure if the pressure is above the threshold value of 0.5 bar and more importantly, the air flow rate at 0.5 bar is indistinguishable between the concretes. To enlarge the difference in flow rates of two concretes, a test pressure 2 bar is recommended for the air permeability measurements.
5) The proposed field test method could be used to measure air permeability of cover concrete, but it should be noted that in order to yield reliable results, the concrete should be in a moisture free condition, such as state equivalent of 21 days of drying in an oven at 40 ^{o}C and this can be assessed by measuring relative humidity, i.e. internal relative humidity of less than 60% in the near-surface region.

Acknowledgement

The experiments described in this paper were carried out in the concrete laboratory of Chongqing University and the authors acknowledge Chongqing University for providing facilities for the investigation reported in this paper. The authors thank financial supports provided by National Natural Science Foundation of China and the Open Research Funds for the Shenzhen University and State Key Laboratory of High Performance Civil Engineering Materials. The support from both the University of Leeds and Queen's University Belfast to complete this manuscript is highly appreciated.

References

Adams, A. E. (1986). Development and application of the CLAM for measureing concrete permeability. PhD thesis, Queen's University Belfast.

Arbaoui, T. (1988). Finite element calibration of the CLAM. MSc, Queen's University Belfast.

Bamforth, P.B. (1987). "The relationship between permeability coefficients for concrete obtained using liquid and gas." Magazine of concrete research, 39 (138): 3-11.

Basheer, P. A. M. (2001). Permeation analysis. Handbook of Analytical Techniques in Concrete Science and Technology: Principles, Techniques and Applications. R. V.S. and J. J. Beaudoin, Noyes Publications: 658-727.

Basheer, P. A. M., D. C. Montgomery and A. Long (1995). "'CLAM' tests for measuring in-situ permeation properties of concrete." NDT & E International 12: 53-73.

BS:1881-125 (1986). Methods for mixing and sampling fresh concrete in the laboratory. London, BSI: 10 pages.

Claisse, P., H. I. Elsayad and I. G. Shaaban (1999). "Test Methods for Measuring Fluid Transport in Cover Concrete." Journal of Materials in Civil Engineering 11(2): 138-143.

Denarie, E., F. Jacobs, A. Leemann, T. Teruzzi and R. T. Torrent (2011). Specification and site control of the permeability of the cover concrete: the Swiss approach. International RILEM Conference on Advances in Construction Materials Through Science and Engineering. C. Leung and K. T. Wan, RILEM Publications SARL: 478 - 485.

Dhir, R. K., P. C. Hewlett, E. A. Brars and I. G. Shaaban (1995). "A new technique for measuring the air permeability of near-surface concrete." Magazine of Concrete Research 47: 167-176.

El-Dieb, A. E. and R. D. Hooton (1995). "water permeability measurement of high performance concrete using a high pressure triaxial cell." Cement and Concrete Research 25: 1199-1208.

Figg, J. W. (1973). "Methods of measuring the air and water permeability of concrete." Magazine of Concrete Research 25: 213-219.

GB/T-50082 (2009). Standard for test methods of long-term performance and durability of ordinary concrete, MOHURD: 51 pages.

Hall, C. (1989). "Water sorptivity of mortars and concretes a review." Magazine of Concrete Research 41: 51-61.

Imamoto, K., K. Shimozawa, N. Nagayama, J. Yamasaki and S. Nimura (2009). Air permeability of concrete cover and its relationship with carbonation progress under long-term exposure test in Japan. Concrete in aggressive aqueous environments - Performance, Testing, and Modeling. M. G. Alexander and A. Bertron, RILEM Publications SARL: 508 - 514.

Neves, R., F. Branco and J. Brito (2011). "About the statistical interpretation of air permeability assessment results." Materials and Structures 45(4): 529-539.

Parrott, L. J. (1994). "Moisture conditioning and transport properties of concrete test specimens." Materials and Structures 27: 460-468.

Parrott, L. J. and C. Z. Hong (1991). "Some factors influecing air permeation measurements in cover conrete." Materials and Structures 24: 403-408.

Rawlings, J. O., S. G. Pantula and D. A. Dickey (1998). Applied regression analysis: A research tool, Springer.

Schonlin, K. and H. K. Hilsdorf (1987). Evaluation of the effectiveness of curing of concrete structures. Concrete Durability: Katharine and Bryant Mather International Conference. J. M. Scanlon, ACI. SP-100: 207-226.

Silva, A., R. Neves and J. de Brito (2014). "Statistical modelling of carbonation in reinforced concrete." Cement and Concrete Composites 50: 73-81.

Torrent, R. T. (1992). "A two-chamber vacuum cell for measuring the coefficient of permeability to air of the concrete cover on site." Materials and Structures 25: 358-365.

Whiting, D. and P. D. Cady (1992). Condition Evaluation of Concrete Bridges Relative to Reinforcement Corrosion. Washington, D.C., Strategic Highway Research Program. Volume 7: Method for field measurement of concrete permeability (SAF): 93.

Yang, K., P. A. M. Basheer, Y. Bai, B. Magee and A. E. Long (2014). "Development of a new in situ test method to measure the air permeability of high performance concretes." NDT & E International 64: 30-40.

Yang, K., P. A. M. Basheer, Y. Bai, B. Magee and A. E. Long (2015-a). "Assessment of the effectiveness of the guard ring in obtaining a uni-directional flow in an in situ water permeability test." Materials and Structures 48(1): 167-183.

Yang, K., P. A. M. Basheer, B. Magee, Y. Bai and A. E. Long (2015-b). "Repeatability and Reliability of New Air and Water Permeability Tests for Assessing the Durability of High-Performance Concretes." Journal of Materials in Civil Engineering 27(12).

Yang, K., P. A. M. Basheer, B. Magee and Y. Bai (2013). "Investigation of moisture condition and Autoclam sensitivity on air permeability measurements for both normal concrete and high performance concrete." Construction and Building Materials 48: 306-314.